European Polymer Journal 46 (2010) 1824–1832

Contents lists available at ScienceDirect

European Polymer Journal

journal homepage: www.elsevier.com/locate/europolj

Macromolecular Nanotechnology

Self-organization of dipeptide-grafted polymeric nanoparticles film: A novel method for surface modification

Jingtian Han [a], Patrick Silcock [a,*], A. James McQuillan [b], Phil Bremer [a]

[a] Department of Food Science, University of Otago, P.O. Box 56, Dunedin, New Zealand
[b] Department of Chemistry, University of Otago, P.O. Box 56, Dunedin, New Zealand

ARTICLE INFO

Article history:
Received 8 November 2009
Received in revised form 18 June 2010
Accepted 23 June 2010
Available online 26 June 2010

Keywords:
Polymer nanoparticles
Self-aggregation
Diblock copolymer
Dipeptide
Alkylated glass surface
Surface modification

ABSTRACT

Novel dipeptide-grafted polymeric nanoparticles were prepared by grafting the dipeptide (Gly-Gly) to a block copolymer backbone, comprised of styrene-alt-(maleic anhydride) and styrene. In aqueous solution PSt_{130}-b-P(St-alt-MAn)$_{58}$-g-GlyGly$_{26}$ formed stable dispersed spherical aggregates of ca. 75 nm. The critical micelle concentration for the dipeptide-grafted block copolymer self-aggregates was 6.3×10^{-3} mg mL^{-1}. The zeta-potential of the aggregates was estimated experimentally. The dispersed polymer nanoparticles effectively self-organized to form stable nanoparticle thin films on hydrophobic solid surfaces, such as octadecyltrichlorosilane modified glass (OTS-G). As the ionic strength and temperature of the polymer suspension increased the surface coverage of the nanoparticle film increased and its hydrophobicity (water contact angle) decreased. Significantly less bovine serum albumin (BSA) adsorbed to nanoparticles modified surfaces with compared OTS-G surfaces. Diglycine grafted polymer nanoparticles have the potential to be used as a novel platform to study protein–protein interactions and to control fouling.

1. Introduction

A key challenge in the production of solid materials with functional properties is the formation of surface coatings, which have a well-organized nanostructure [1]. Layer-by-layer (LBL) techniques utilizing electrostatic and hydrogen-bonding interactions have been used to build multilayer thin films that possess different functionalities, structure and composition [2–5]. Within this class of films amphiphilic block copolymer micelles have frequently been used as molecular building blocks to allow the formation of nanostructured surface films [6,7]. Using LBL techniques polymeric micelles have been investigated for applications such as the production of nanocapsules [7,8] or anti-reflective films [9] and for producing nanostructured coating for surface modification [10]. To build LBL thin films through electrostatic interactions a charged substrate is necessary which can potentially limit film stability as disassembly can occur due to changes in pH or ionic strength [11,12]. The use of hydrophobic interactions presents an opportunity to produce defined thin film, on non-charged hydrophobic substrates, which have a high stability against changes in pH and ionic strength. Hydrophobic interactions are mainly responsible for the affinity between a hydrophobic solid surface and amphiphilic molecules, such as surfactants, in solution. This affinity has been used to prepare ordered molecular films of surfactants and polymers on hydrophobic solid surfaces at solid–solution interfaces [13,14]. For example, PEO-PPO-PEO block polymers have been shown to form stable films on hydrophobic surfaces [15,16]. Cationic and anionic surface charged polystyrene particle latexes in aqueous suspensions have also been used to form self-organized, dispersed-type and aggregated monolayers on hydrophobic solid substrates via hydrophobic interactions [17,18]. The adsorption kinetics and rearrangement of poly(*tert*-butylstyrene-b-sodium-4-styrenesulfonate) (PtBSNaPSS) diblock copolymer micelles at the solid–liquid interface was also reported [19].

* Corresponding author. Fax: +64 3 4 797567.
E-mail address: pat.silcock@otago.ac.nz (P. Silcock).

0014-3057/$ - see front matter © 2010 Elsevier Ltd. All rights reserved.
doi:10.1016/j.eurpolymj.2010.06.007

As proteins are the main functional components necessary for cell adhesion [20] there is great interest effort in designing protein or peptides grafted polymer surfaces to investigate specific cell–surface interactions. Recently modified surfaces of Arg-Gly-Asp- (RGD) and Arg-Asp-Gly- (RDG) grafted copolymer poly(L-lysine)-g-poly(ethylene glycol) (PLL-g-PEG) [21,22] were shown to efficiently block the adsorption of serum proteins to Nb_2O_5, TiO_x and tissue culture polystyrene while specifically supporting attachment and spreading of human dermal fibroblasts and to further reduce plasma protein adsorption. Further cell adhesion peptide-(YRGDS, YEILDV)-modified poly(ethylene glycol) grafted poly(acrylic acid) PEG-g-PA copolymers significantly reduced protein adsorption [23]. In order to develop novel materials to inhibit random protein fouling and bacterial adhesion, a Gly-Gly dimer was used as model peptide for the preparation of peptide modified PSt_{130}-b-P(St-alt-MAn)$_{58}$-g-$GlyGly_{26}$ copolymer coating. Gly-Gly was selected, as it is stable, commercially available, inexpensive, has a simple chemical composition and a well-characterized structure.

In this work, we present a new, simple route for the preparation of novel surface films of diglycine-grafted polymeric nanoparticles on hydrophobic solid surface via self-organization through hydrophobic interactions. The novel PSt_{130}-b-P(St-alt-MAn)$_{58}$-g-$GlyGly_{26}$ polymeric nanoparticles were produced by grafting, in a one-pot reaction, Gly-Gly dipeptides to a polymer backbone comprising of polystyrene and poly(styrene-alt-maleic anhydride) blocks (Scheme 1). In aqueous solution this grafted amphiphilic polymer self-assembled to form monodispersed micelle-like spherical nanoparticles which effectively self-organized onto a hydrophobic solid surface of octadecyltrichlorosilane modified glass (G-OTS), The nanoparticle modified G-OTS surface showed significantly reduced protein adsorption. The wettability, the surface properties and the morphologies of the resulting polymer nanoparticle thin films are reported and discussed.

2. Experimental

2.1. Materials

Polystyrene$_{130}$-b-poly(styrene-alt-maleic anhydride)$_{58}$ block copolymer (PSt_{130}-b-P(St-alt-MAn)$_{58}$, *Mn* = 25.3 kDa, polydispersity PDI = 1.33) was synthesized via radical addition fragmentation chain transfer (RAFT) copolymerization and characterized as described previously [24].

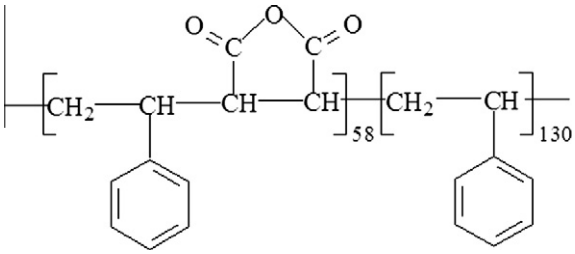

Scheme 1. Structure of P(St-alt-MAn)$_{58}$-b-PSt_{130} block copolymer.

Dipeptide Gly-Gly was obtained from Sigma, USA. Octadecyltrichlorosilane (OTS) and glass beads (d = 150–202 μm) were purchased from Sigma–Aldrich (Australia). Microscope glass slides (25 × 75 × 1 mm) were obtained from Biolab Scientific Ltd. (Australia). All the solvents used in this study were analytical or HPLC grade. Water used was deionised water ((Milli-Q®, 18.2 MΩ, TOC:<20 ppb, Millipore).

2.2. Synthesis of dipeptide-grafted polymeric nanoparticles

PSt_{130}-b-P(St-alt-MAn)$_{58}$-g-$GlyGly_{26}$ was prepared by the drop wise (about 0.01 mL every 10 s using a microsyringe) addition of 5.0 mL containing 0.218 g P(St-alt-MAn)$_{58}$-b-PSt_{130} copolymer (0.50 mmol MAn units) in DMF into 100 mL of Gly-Gly (0.33 g, 2.5 mmol) solution containing 5 mmol (0.68 mL) of triethylamine (TEA). The Gly-Gly solution was cooled at 0 °C in an ice bath prior and during the addition of polymer solution. The nanoparticle suspension was stirred intensively during copolymer addition and for a further 24 h, then dialyzed against water for 7 days. The nanoparticle suspension was freeze dried, the solids level determined and the nanoparticles stored until required for evaluation.

2.3. Preparation of alkylated glass substrate

Prior to silanization, glass substrates were submerged in a freshly prepared mixture of H_2SO_4 (98%) and H_2O_2 (30%) at a volume ratio of 7:3 for 1 h at 80 °C and then the samples were rinsed thoroughly with pure water and dried using a N_2 gas stream. The freshly cleaned glass substrates were dipped into 1% solution of silane coupling agents OTS in anhydrous toluene at room temperature for 24 h, followed by washing with toluene and drying under vacuum.

2.4. Self-organization of polymer particles on alkylated glass substrates

Self-organization of the polymeric nanoparticles onto alkylated glass substrates was carried out as follows: alkylated glass slides or beads were immersed into a polymer nanoparticle dispersion (pH 6.5) at a given concentration for 24 h, then removed from the dispersion and washed with water in an ultrasonic bath for 5 min to remove weakly adsorbed particles. The morphology of the polymer nanoparticle films was observed by SEM. Characterization of the modified hydrophobic glass surface was carried out by contact angle measurements of deionised water.

2.5. Characterization of Gly-Gly grafted copolymer

Infrared spectra were recorded using a DigiLab FTS 4000 spectrometer. ^{1}H NMR spectra were recorded on a 500 MHz Oxford 500 spectrometer and samples were prepared at concentrations of 10 mg mL^{-1} in DMSO-d_6. *Elemental analysis* was performed by the Campbell Microanalytical Laboratory, Department of Chemistry, University of Otago, using a Carlo Erba 1108 Elemental Analyzer.

2.6. Measurements of self-assembled PSt_{130}-b-P(St-alt-MAn)$_{58}$-g-GlyGly$_{26}$ nanoparticles

The size distribution of the dipeptide-grafted polymeric nanoparticles was measured at 25 °C using a *dynamic laser light scattering instrument* (DLS, HPP5001 Malvern Instruments Ltd., UK) equipped with a He–Ne laser with a scattering angle of 90°. The particle size and size distribution were calculated using non-negative least squares algorithms [25,26]. Prior to the particle size measurements, the polymer suspensions (0.1 mg mL^{-1}) were sonicated for 2 min and passed through a 0.45 μm filter (Millipore). The zeta-potentials and the Debye plot of the self-assembled polymeric nanoparticles were determined using a Zetasizer Nano ZS (Malvern Instruments Ltd., UK) at 25 °C. The pH of the nanoparticle suspensions (0.1 mg mL^{-1}) was adjusted with either NaOH or HCl solutions. The Debye plots were obtained using *static light scattering* (SLS) in the polymer concentration ranges from 0.2 to 0.7 mg mL^{-1} at a pH 6.5. The measurements of the differential refractive index increment d*n*/d*c* of the nanoparticle suspensions were made with an Abbe Refractometer. The morphology of the nanoparticles was observed using a *transmission electron microscope* (TEM) according to the method published [26]. A drop of nanoparticle suspension containing 0.1% phosphotungstic acid (PTA) was placed onto a copper grid coated with carbon film and dried at room temperature. Observation was performed at 80 kV with a Philips EM CM100 TEM. The fluorescence spectra were recorded on a *spectrofluorophotometer* (LS50B Fluorimeter, Perkin-Elmer).

2.7. Characterization of PSt_{130}-b-P(St-alt-MAn)$_{58}$-g-GlyGly$_{26}$ nanoparticles thin film on G-OTS surface

The surface morphology of the grafted block copolymer nanoparticles modified OTS-G was examined using a JEOL 6700F Field Emission *Scanning Electron Microscope* (JEOL, Japan). Samples were sputter coated with approximately 5 nm of Cr in an Emitech K250 coating attachment (Emitech, UK). Samples were viewed and imaged at 3 kV using a LEI detector. *Contact angle* were measured using a First Ten Angstroms contact angle instrument (FTA 200) at room temperature. The system consists of a measurement platform and a frame grabber (video capture) card running in a personal computer.

2.8. Protein adsorption study

To determine the protein adsorption to the various solid surfaces, OTS-G or PSt_{130}-b-P(St-alt-MAn)$_{58}$-g-GlyGly$_{26}$ coated OTS-G beads (G-OTS-Polym, 500 mg) were hydrated in 10 mL phosphate buffer (50 mM, pH 7.4) for 10 min. The suspension was centrifuged (1090 g, 10 min, 20 °C) and 9.0 mL of supernatant removed. Protein solutions with varying concentration of BSA from 0.05 to 0.5 mg mL^{-1} in 50 mM phosphate buffer (pH 7.4) were added to the hydrated glass beads and the suspension tumbled for 20 h at 20 °C. The amount of protein adsorbed to the substrates was determined by measuring the protein remaining in the solution by the Bradford method [27].

3. Results and discussion

3.1. Preparation and characterization of dipeptide-grafted polymeric nanoparticles

The composition of the dipeptide grafted copolymer was determined by elemental analysis (Table 1), calculated from the signal area of ^{1}H NMR and ^{13}C NMR [24] and was expressed as PSt_{130}-b-P(St-alt-MAn)$_{58}$-g-GlyGly$_{26}$. The grafting degree (GD) was calculated to be 44.8% in molar percent of the total units of maleic anhydride groups in polymer backbone. The IR spectrum of the Gly-Gly grafted amphiphilic block copolymer of PSt_{130}-b-P(St-alt-MAn)$_{58}$-g-GlyGly$_{26}$ (Fig. 1) showed that the anhydride peaks at 1776 and 1854 cm^{-1}, present in the polymer backbone PSt_{130}-b-P(St-alt-MAn)$_{58}$ had been replaced by absorptions at 1710, 1412, 1561, 1647 and 1548 cm^{-1}. The bands present at 1647 cm^{-1} (amide I, mainly C═O stretch) and 1548 cm^{-1} (amide II, mainly N—H bond, overlapped with peak of 1561 cm^{-1}) [28–30], clearly showed that the dipeptide, Gly-Gly, had been successfully grafted onto the polymer PS_{130}-b-P(St-alt-MAn)$_{58}$. The absorptions at 1710 cm^{-1} (carbonyl stretch, C═O, of carboxylic acid), 1412 and 1561 cm^{-1} (symmetric and antisymmetric stretching frequencies of carboxylate ion, COO^-, respectively) showed that the formation of carboxylate groups had also occurred [31]. The presence of peaks 1452 and 1492 cm^{-1} in the spectra of copolymers before and after Gly-Gly grafting was assigned to the stretching vibration of the carbon–carbon bonds in the benzene rings of polystyrene [32].

The grafted amphiphilic block copolymer formed micelle-like aggregates in aqueous medium. The aggregates were purified by dialysis against deionised water. DLS studies showed that the aggregated polymers formed polymeric nanoparticles with a hydrodynamic diameter distribution $f(D_h)$ in the range of 70–80 nm (average ca. 75 nm) at 25 °C in water at pH 6.5 (Fig. 2) and remained relatively constant over copolymer concentration ranges of

Table 1
Elemental analysis of the block copolymers based on maleic anhydride and styrene.

Elements	P(St-alt-MAn)$_{58}$-b-PSt$_{130}$		PSt_{130}-b-P(St-alt-MAn)$_{58}$-g-GlyGly$_{26}$	
	Measured (%)	Calculated (%)	Measured (%)	Calculated (%)
C	82.46 ± 0.02	82.55	75.09 ± 0.08	75.17
H	6.46 ± 0.06	6.42	6.55 ± 0.14	6.44
O	11.09 ± 0.08	11.03	15.84 ± 0.11	15.91
N			2.52 ± 0.03	2.48

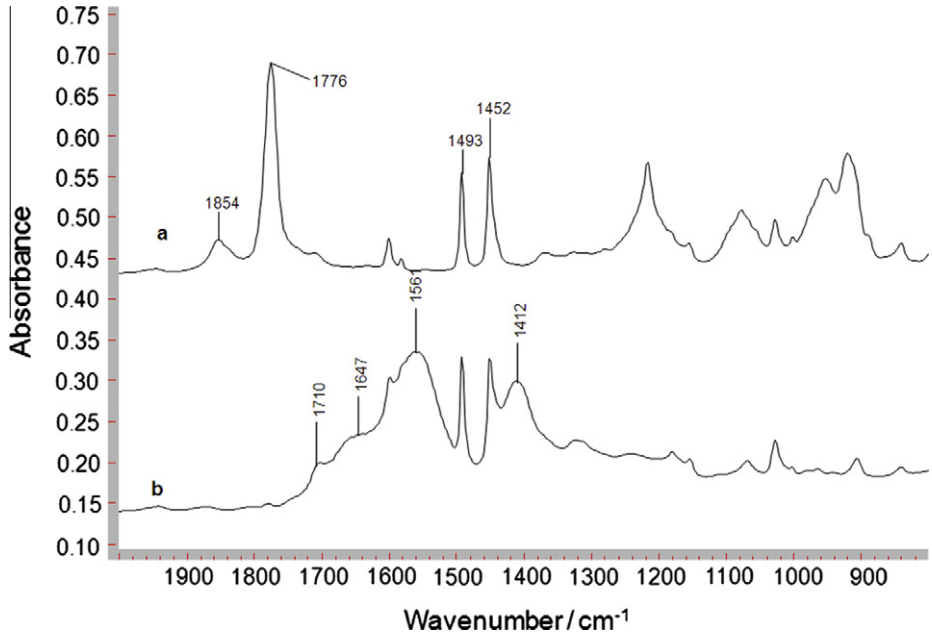

Fig. 1. ATR-IR spectra of (a) P(St-alt-MAn)$_{58}$-b-PSt$_{130}$ and (b) the dipeptide Gly-Gly grafted amphiphilic polymer PSt$_{130}$-b-P(St-alt-MAn)$_{58}$-g-GlyGly$_{26}$.

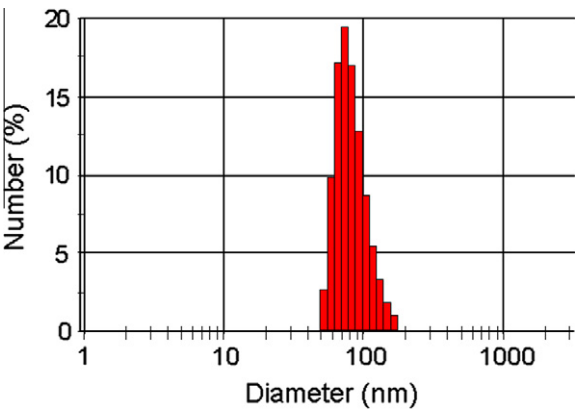

Fig. 2. Particle size distribution of PSt$_{130}$-b-P(St-alt-MAn)$_{58}$-g-GlyGly$_{26}$ polymeric nanoparticle.

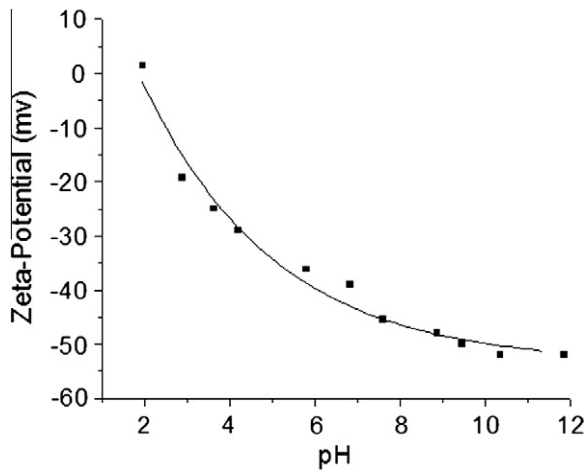

Fig. 3. Effect of pH on zeta-potential of PSt$_{130}$-b-P(St-alt-MAn)$_{58}$-g-GlyGly$_{26}$ polymeric nanoparticle in 1.0 mM NaCl solution at 25 °C.

0.05–1.0 mg mL^{-1}. The hydrodynamic diameter of the particles did not change significantly after 6 months storage at 4 °C (data not shown). The effect of pH on the charge of the dipeptide-grafted polymer nanoparticles was determined by measuring their zeta-potential in 1.0 mM NaCl solution at 25 °C. The isoelectric point of the PSt$_{130}$-b-P(St-alt-MAn)$_{58}$-g-GlyGly$_{26}$ nanoparticles was approximately pH 2.0 (0 mV). Above this pH, the polymer nanoparticles carried a net negative charge with the zeta-potential decreasing to −55 mV at pH 12 due to the dissociation of the carboxylic acid groups. A titration of the zeta-potential of the micelles as a function of pH is shown in Fig. 3. The strong negative charge is believed to contribute to the nanoparticles stability as the strong electrostatic repulsion will create a high electrostatic energy barrier and minimize particle aggregation [33]. The Debye plots of the polymer nanoparticle suspensions were obtained using static light scattering (SLS) in water at pH 6.5. Based on the differential refractive index increment dn/dc (0.173 mL/g) measured with an Abbe Refractometer, the weight-average molar mass was calculated as 7.07×10^6 g/mol, and the apparent aggregation number N^{agg} as 241 .

TEM images of the core–shell nanoparticles showed that the aggregates were spheres with diameters of approximately 57 ± 6 nm (Fig. 4). In comparison the D_h of the nanoparticles, as measured by DLS, were about 75 nm. This difference in estimated diameter is due to the particles swelling in the presence of water (D_h measurements) and the collapse of the free hydrophilic segments of the polymer as well as the dehydration of the polymer chains as dried in preparation for TEM observation [34].

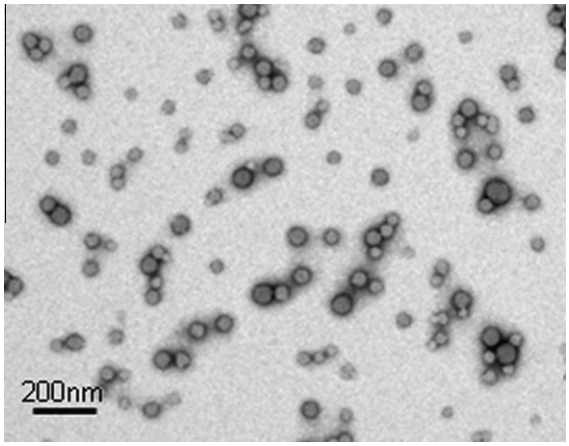

Fig. 4. TEM image of PSt_{130}-b-P(St-alt-MAn)$_{58}$-g-$GlyGly_{26}$ nanoparticles with 0.1% PTA negative staining.

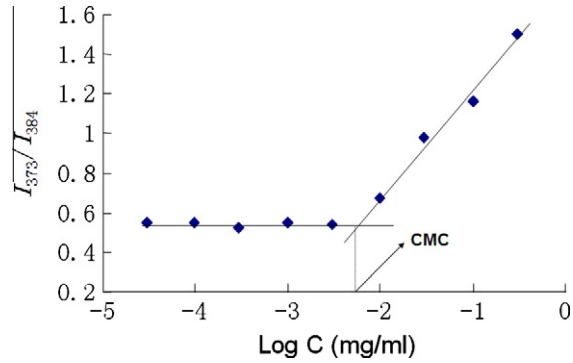

Fig. 5. Intensity ratio (I_{373}/I_{384}) of pyrene from the emission spectra as a function of the concentration of PSt_{130}-b-P(St-alt-MAn)$_{58}$-g-$GlyGly_{26}$ solution.

The formation of micelle-like aggregates which had a PSt hydrophobic domain (core) and P(St-alt-MAn)-g-Gly-Gly exterior hydrophilic corona (or shell) was verified by a fluorescence probe technique using pyrene as described by Choi [35]. The emission fluorescence spectra were recorded on a spectrofluorophotometer with an excitation wavelength of 340 nm and a 5 nm bandwidth. I_1 and I_3 are the fluorescence intensities of pyrene spectrum at 373 and 384 nm. The ratio of I_1 to I_3 reflects the polarity of microenvironment around the pyrene [36,37]. Fig. 5 shows the intensity (peak height) ratio I_{373}/I_{384} as a function of the polymer concentration. The fluorescence intensity ratio I_{373}/I_{384} was approximately constant when the concentration of the grafted block copolymer was below 6.3×10^{-3} mg mL^{-1}. This ratio increased dramatically as the concentration increased above this point, indicating the formation of micelle-like nanoparticles and the transfer of pyrene into the hydrophobic cores of the nanosphere. This concentration was defined as the critical micelle concentration (CMC) [36,38,39]. The CMC value for the PSt_{130}-b-P(St-alt-MAn)$_{58}$-g-$GlyGly_{26}$ nanoparticles was about sixfold higher than that for the amphiphilic block copolymer (PSt_{130}-b-P(St-alt-MA)$_{58}$) nanoparticles (CMC = 1.0×10^{-3} mg mL^{-1}) hydrolyzed from polymer backbone PSt_{130}-b-P(St-alt-MAn)$_{58}$ [24]. Both of these amphiphilic copolymers possessed the same length of hydrophobic PSt_{130} segments. However, the grafting of Gly-Gly increased the hydrophilic segments of P(St-alt-MAn)$_{58}$-g-$GlyGly_{26}$ compared to P(St-alt-MA)$_{58}$. This result is inline with other studies where, for a constant length of the core forming block, increasing the length of the hydrophilic block increased the CMC value [40–42].

3.2. Self-organization of dipeptide-grafted polymeric nanoparticles on alkylated glass surfaces

Alkylated glass substrate (OTS-G) was immersed into PSt_{130}-b-P(St-alt-MAn)$_{58}$-g-$GlyGly_{26}$ suspension (0.25 mg mL^{-1}, pH 6.5) at 60 °C for 24 h. After cleaning in water by ultrasonic bath, a stable polymer nanoparticle film was formed on the hydrophobic substrate through hydrophobic interactions. SEM images of the OTS-G surface and nanoparticle film show that the polymer nanoparticles are effectively self-organized on the alkylated solid surface to form an aggregated-type monolayer (Fig. 6), which appears similar to the film formed by the self-organization of cationic polystyrene latex onto the OTS-G substrate [16].

The relationship between the concentration of the nanoparticle suspension and the polymeric films on OTS-G plates is shown in Fig. 7. As the PSt_{130}-b-P(St-alt-MAn)$_{58}$-g-$GlyGly_{26}$ nanoparticle concentration in suspension increased the morphology of the films on the modified OTS-G changed. At lower nanoparticle concentrations of 0.01 and 0.025 mg mL^{-1}, the modified OTS-G surface (Fig. 7a and b) was relatively featureless and smooth. As the nanoparticle concentration was increased to 0.05 and 0.10 mg mL^{-1} the surfaces contained more obvious features and they appeared to be rougher (Fig. 7c and d). At concentrations higher than 0.20 mg mL^{-1}, stable aggregated-type nanoparticle films were formed (Fig. 7e and f). Overall adsorption of the nanoparticle to the surface appears to result in the nanoparticles restructuring to minimize contact between the hydrophobic surface and water [13,14]. At low concentrations the nanoparticles spread to maximize surface coverage. At higher nanoparticle concentrations hydrophobic interactions also occurred between nanoparticles resulting in particle–particle coalescence on the surface and the formation of an "aggregated-type" nanoparticle film. These results are in agreement with those of Boxshall [15] and McGurk [16] who report a film of aggregates was formed at concentrations higher than the CMC when using PEO-PPO-PEO. In contrast to those results the Gly-Gly modified nanoparticle films appeared to form stable films that were not removed by the rinsing and sonicating pre-treatment. This may have been due to the greater hydrophobicity of the PS block in the Gly-Gly grafted nanoparticle compared to the PPO bock in the PEO-PPO-PEO aggregates.

Water contact angles were used to characterize the relative hydrophilicity or hydrophobicity [43] of the polymer nanoparticle suspension modified OTS-S substrates. As the concentration of the nanoparticle suspension was increased to about 0.50 mg mL^{-1} the contact angle of the nanoparticle modified hydrophobic surfaces decreased. At

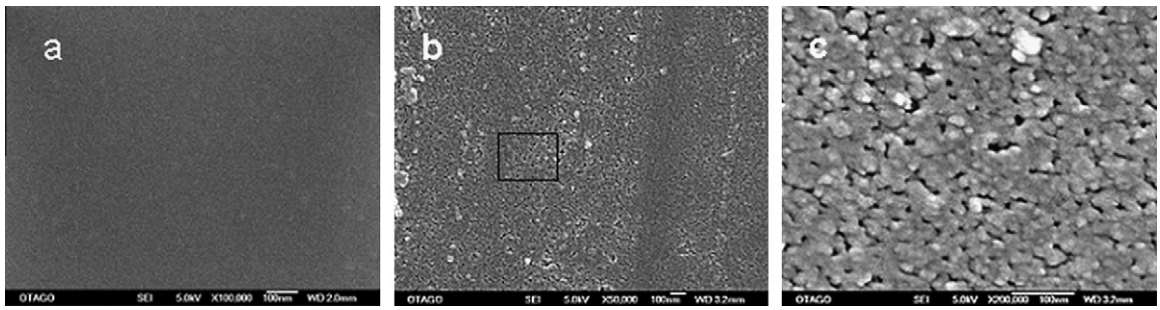

Fig. 6. Scanning electron microscope (SEM) image of OTS-G (a) and self-organized PSt_{130}-b-P(St-alt-MAn)$_{58}$-g-$GlyGly_{26}$ nanoparticles film (0.25 mg mL^{-1}) on OTS-G (adsorption time and temperature 24 h and 60 °C, respectively) (b) 50,000× (c) 200,000×.

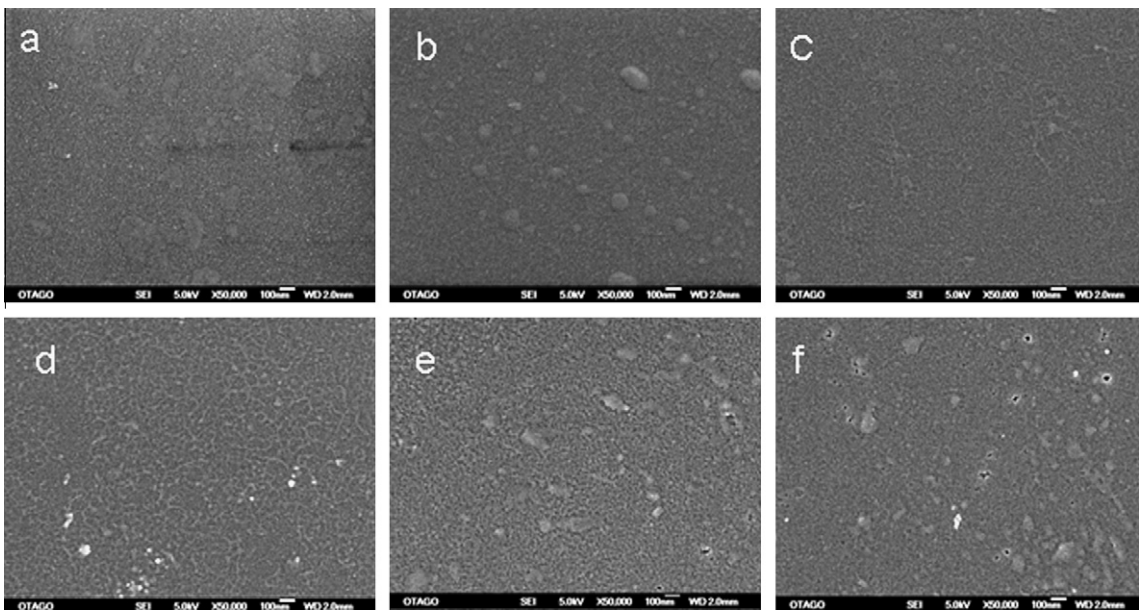

Fig. 7. SEM images of nanoparticles self-organized on OTS-G with different concentrations of polymer suspension at 60 °C for 24 h. (a) 0.01, (b) 0.025, (c) 0.05, (d) 0.10, (e) 0.20 and (f) 0.50 mg mL^{-1}. (Magnification: 50,000×).

concentrations greater than 0.50 mg mL^{-1} the contact angle remained constant at about 70° (Fig. 8). The decrease in contact angle with increasing nanoparticle concentration was attributed to the surface coverage of the hydrophilic P(St-alt-MAn)$_{58}$-g-$GlyGly_{26}$ nanoparticles on the OTS-G surface increasing which, as well as decreasing the hydrophobicity also increased the surface roughness.

The impact of variations in ionic strength and temperature on the surface properties of the charged polymer nanoparticles were considered in light of their predicted impact on the nanoparticles electric double layer [16]. As the NaCl concentration increased, the electrostatic repulsion between the polymeric nanoparticles decreased resulting in a decrease in the water contact angle until a plateau value was obtained at about 250 mM (Fig. 9).

For PSt_{130}-b-P(St-alt-MAn)$_{58}$-g-$GlyGly_{26}$ nanoparticles on OTS-G, the contact angle slowly decreased from 92° to 69° as the incubation temperature of the nanoparticle

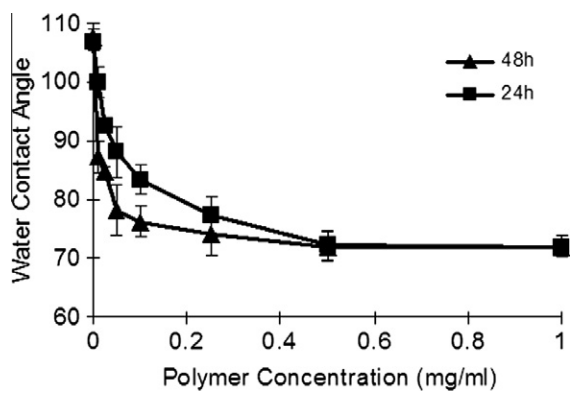

Fig. 8. The influence of polymer concentration on static water contact angles of the nanoparticle assembled OTS-G substrates after adsorption for 24 and 48 h at 60 °C. Bars represent the mean of 10 measurements ±SD.

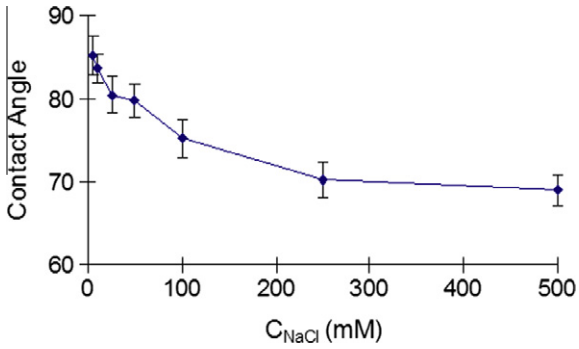

Fig. 9. Contact angles of the self-organized PSt_{130}-b-P(St-alt-MAn)$_{58}$-g-$GlyGly_{26}$ nanoparticle film adsorbed onto the OTS-G plates in the presence of NaCl, polymer concentration of 0.2 mg mL^{-1}, adsorption temperature 60 °C and adsorption time 24 h. Bars represent the mean of 10 measurements ±SD.

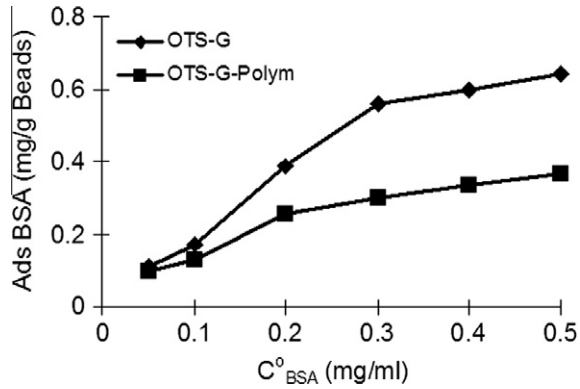

Fig. 11. The amount of adsorbed BSA on the PSt_{130}-b-P(St-alt-MA)$_{58}$-g-$GlyGly_{26}$ nanoparticles film coated OTS-G beads in phosphate buffer (50 mM, pH 7.4) at 20 °C for 24 h.

suspension (0.20 mg mL^{-1}) in the presence of the OTS-G surface increased from 20 to 80 °C. This decrease is suggested to be due to the higher temperature increasing the rate of Brownian motion and hence the number of particle collisions against the hydrophobic substrate, resulting in an increase in surface coverage and decrease in water contact angle [17]. A further dramatic decrease in contact angle to 32° was observed when the temperature was increased to 100 °C (Fig. 10). This abrupt change is believed to be due to the transition of the polystyrene (PSt_{130}) core in the self-assembled nanoparticles from a glassy to rubbery state as the Tg of 92 °C [24] was exceeded [44,45]. This would increase the coverage of the polymer nanoparticles and decrease the water contact angle as the rubbery state enables greater movement and restructuring of the nanoparticles so as to minimize the hydrophilic–hydrophobic repulsions and maximize exposure of the hydrophilic groups to water.

3.3. Protein adsorption

The nanoparticle modified alkylated glass reduced BSA adsorption compared to adsorption onto the OTS-G surfaces, with the magnitude of difference between the amount of protein adsorbed onto the two surfaces increasing as the amount of BSA in solution increased (Fig. 11). The reduction in the protein adhesion was likely due to the increased negative charge and the increased hydrophilicity of the nanoparticle-modified surface [46,47].

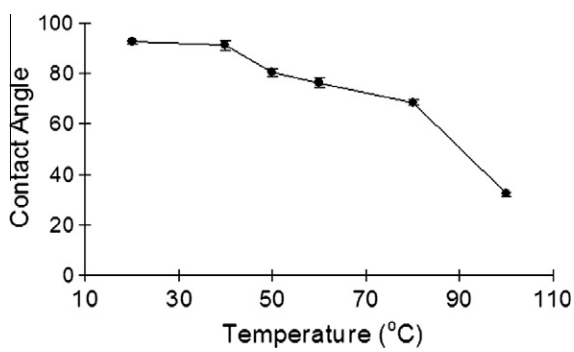

Fig. 10. Effect of temperature on the contact angle of self-organized PSt_{130}-b-P(St-alt-MAn)$_{58}$-g-$GlyGly_{26}$ nanoparticle films adsorbed onto OTS-G plates. OTS-G plates were immersed in the polymer nanoparticle suspension (0.20 mg mL^{-1}) containing 100 mM NaCl for 24 h at defined temperature. Bars represent the mean of 10 measurements ±SD.

The results suggest that top-down assembly of thin films can be achieved using nanoparticles. Using the Gly-Gly-modified nanoparticles and controlling temperature and ionic strength during adsorption it was possible to fine-tune the film coverage and functionality. These films have the potential to be used to reduce bacterial adhesion or protein adsorption. Further, grafting the block polymer with specific antifouling peptides, e.g. RDG, may allow further modifications to the film functionality to be made. Such films could also be used as a novel platform for the study of protein–protein interactions and may have applications in the fields of biofouling control or biosensor development.

4. Conclusions

Novel amphiphilic micelle-like polymer nanoparticles, PSt_{130}-b-P(St-alt-MAn)$_{58}$-g-$GlyGly_{26}$, were prepared by grafting Gly-Gly to a block copolymer based on maleic anhydride and styrene. The core–shell polymer nanoparticles effectively self-organized on hydrophobic solid substrates through hydrophobic interactions to form stable films, with the surface morphology being most dependent on the concentration of the nanoparticles suspension. At lower polymer concentrations, the surface appeared to be smooth and featureless. As polymer concentration increased a stable aggregated-type, nanoparticle film was formed. The nanoparticle film significantly reduced BSA adsorption. The results suggest that such films may have the potential to be used for surface modification and to prepare nanostructured antifouling surface coatings.

Acknowledgment

This research was funded by the New Zealand Foundation for Research, Science and Technology (Contract

CO8X0409, Multiscale Modelling Programme). The authors thank Liz Girvan and the Otago Centre for Electron Microscopy (OCEM) for assistance with electron microscopy.

References

[1] Sakai K, Webber GB, Vo C-D, Wanless EJ, Vamvakaki M, Butun V, et al. Characterization of layer-by-layer self-assembled multilayer films of diblock copolymer micelles. Langmuir 2008;24:116–23.

[2] Wang F, Wang G, Yang S, Li C. Layer-by-layer assembly of aqueous dispersible, highly conductive poly(aniline-co-*o*-anisidine)/poly(sodium 4-styrenesulfonate)/MWNTs core–shell nanocomposites. Langmuir 2008;24:5825–31.

[3] Morgan SE, Jones P, Lamont AS, Heidenreich A, McCormick CL. Layer-by-layer assembly of pH-responsive, compositionally controlled (co)polyelectrolytes synthesized via RAFT. Langmuir 2007;23: 230–40.

[4] Marletta A, Silva RA, Ribeiro PA, Raposo M, Goncalves D. Modeling adsorption processes of poly-*p*-phenylenevinylene precursor and sodium acid dodecylbenzenesulfonate onto layer-by-layer films using a Langmuir-type metastable equilibrium model. Langmuir 2009;25:2166–71.

[5] Cai K, Rechtenbach A, Hao J, Bossert J, Jandt KD. Polysaccharide–protein surface modification of titanium via a layer-by-layer technique: characterization and cell behaviour aspects. Biomacromolecules 2005;26:5960–71.

[6] Zapotoczny S, Golonka M, Nowakowska M. Nanostructured micellar films formed via layer-by-layer deposition of photoactive polymer. Langmuir 2008;24:5868–76.

[7] Ma N, Zhang H, Song B, Wang Z, Zhang X. Polymer micelles as building blocks for layer-by-layer assembly: an approach for incorporation and controlled release of water-insoluble dyes. Chem Mater 2005;17: 5065–96.

[8] Addison T, Cayre OJ, Biggs S, Armes SP, York D. Incorporation of block copolymer micelles into multilayer films for use as nanodelivery systems. Langmuir 2008;24:13328–33.

[9] Cho J, Hong J, Char K, Caruso F. Nanoporous block copolymer micelle/micelle multilayer films with dual optical properties. J Am Chem Soc 2006;128:9935–42.

[10] Sruanganurak A, Sanguansap K, Tangboriboonrat P. Layer-by-layer assembled nanoparticles: a novel method for surface modification of natural rubber latex film. Colloids Surf A Physicochem Eng Aspects 2006;289:110–7.

[11] Amigoni S, Givenchy ETd, Dufay M, Guittard F. Covalent layer-by-layer assembled superhydrophobic organic–inorganic hybrid films. Langmuir 2009;25:11073–7.

[12] Quinn JF, Johnston APR, Such GK, Zelikin AN, Caruso F. Next generation, sequentially assembled ultrathin films: beyond electrostatics. Chem Soc Rev 2007;36:707–18.

[13] Somasundaran P, Krishnakumar S. Adsorption of surfactants and polymers at the solid–liquid interface. Colloids Surf A Physicochem Eng Aspects 1997;123–124:491–513.

[14] Grant LM, Ducker WA. Effect of substrate hydrophobicity on surfactant surface-aggregate geometry: zwitterionic and nonionic surfactants. J Phys Chem 1997;101:5337–45.

[15] Keir Boxshall K, Wu M-H, Cui Z, Cui Z-F, John F, Watts JF, et al. Simple surface treatments to modify protein adsorption and cell attachment properties within a poly(dimethylsiloxane) micro-bioreactor. Surf Interface Anal 2006;38:198–201.

[16] McGurk SL, Green RJ, Sanders GHW, Davies MC, Roberts CJ, Tendler SJB, et al. Molecular interactions of biomolecules with surface-engineered interfaces using atomic force microscopy and surface plasmon resonance. Langmuir 1999;15:5136–40.

[17] Watanabe M, Kawaguchi S, Nagai K. Self-organization of polymer particles on hydrophobic solid substrates in aqueous media. I. Self-organization of cationic polymer particles on alkylated glass plates. Colloid Polym Sci 2006;285:305–14.

[18] Yamaguchi K, Taniguchi T, Kawaguchi S, Nagai K. Novel self-organization of polymer particles on hydrophobic solid surfaces through hydrophobic interaction. Colloid Polym Sci 2004;282:684–92.

[19] Ryan Toomey R, Mays J, Yang J, Tirrell M. Postadsorption rearrangements of block copolymer micelles at the solid/liquid interface. Macromolecules 2006;39:2262–7.

[20] Chen H, Yuan L, Song W, Wu Z, Li D. Biocompatible polymer materials: role of protein–surface interactions. Prog Polym Sci 2008;33:1059–87.

[21] VandeVondele S, Voros J, Hubbell JA. RGD-grafted poly-L-lysine-grafte-(polyethylene glycol) copolymers block non-specific protein adsorption while promoting cell adhesion. Biotechnol Bioeng 2003;82:784–90.

[22] Hansson Kenny M, Tosattic S, Isakssond J, Wettero J, Textorc M, Lindahlf TL, et al. Whole blood coagulation on protein adsorption-resistant PEG and peptide functionalised PEG-coated titanium surfaces. Biomaterials 2005;26:861–72.

[23] Wagner VE, Jeffrey T, Koberstein JT, James D, Bryers JD. Protein and bacterial fouling characteristics of peptide and antibody decorated surfaces of PEG-poly(acrylic acid) co-polymers. Biomaterials 2004;25:2247–63.

[24] Han J, Silcock P, McQuillan AJ, Bremer P. Preparation and characterization of poly(styrene-alt-maleic acid)-b-polystyrene block copolymer self-assembled nanoparticles. Colloid Polym Sci 2008;286:1605–12.

[25] Jeong JH, Cho YW, Jung B, Park K, Kim J-D. Self-assembled nanoparticles of ribozymes with poly(ethylene glycol)-b-poly(L-lysine) block copolymers. Jpn. J. Appl. Phys. Part 1: regular papers. Brief Commun Rev Pap 2006;45:591–5.

[26] Jeong JH, Kang HS, Yang SR, Kim J-D. Polymer micelle-like aggregates of novel amphiphilic biodegradable poly(asparagine) grafted with poly(caprolactone). Polymer 2003;44:583–91.

[27] Bradford MM. A rapid and sensitive method for the quantitation of microgram quantities of protein utilizing the principle of protein-dye binding. Anal Biochem 1976;72:248–54.

[28] Jia Z, Du S, Tian G. Surface modification of acrylic fiber by grafting of casein. J Macromol Sci A Pure Appl Chem 2007;44:299–304.

[29] Kang S-Y, Bremer PJ, Kim K-W, McQuillan AJ. Monitoring metal ion binding in single-layer *Pseudomonas aeruginosa* biofilms using ATR-IR spectroscopy. Langmuir 2006;22:286–91.

[30] Jiang W, Saxena A, Song B, Ward BB, Beveridge TJ, Myneni SCB. Elucidation of functional groups on Gram-positive and Gram-negative bacterial surfaces using infrared spectroscopy. Langmuir 2004;20:11433–42.

[31] Kirwan LJ, Fawell PD, Bronswijk Wv. In situ FTIR-ATR examination of poly(acrylic acid) adsorbed onto hematite at low pH. Langmuir 2003;19:5802–7.

[32] Branan N, Wells TA. Microorganism characterization using ATR-FTIR on an ultrathin polystyrene layer. Vib Spectrosc 2007;44:192–6.

[33] Kallay N, Zalac S. Stability of nanodispersions: a model for kinetics of aggregation of nanoparticles. J Colloid Interface Sci 2002;253:70–6.

[34] Zhang W, Shi L, Ma R, An Y, Xu Y, Wu K. Micellization of thermo- and pH-responsive triblock copolymer of poly(ethylene glycol)-b-poly(4-vinylpyridine)-b-poly(*N*-isopropylacrylamide). Macromolecules 2005;38:8850–2.

[35] Choi CY, Chae SY, Kim J-D, Jang M-K, Cho CS, Nah J-W. Preparation and characterizations of poly(ethylene glycol)-poly(ε-caprolactone) block copolymer nanoparticles. Bull Korean Chem Soc 2005;26:523–8.

[36] Yang Z, Zhang W, Liu J, Shi W. Synthesis of amphiphilic poly(ether-amide) dendrimer endcapped with poly(ethylene glycol) grafts and its solubilization to salicylic acid. Colloid Surf B Biointerfaces 2007;55:229–34.

[37] Brahma A, Mandal C, Bhattacharyya D. Characterization of a dimeric unfolding intermediate of bovine serum albumin under mildly acidic condition. Biochim Biophys Acta 2005;1751:159–69.

[38] Soppimath KS, Tan DCW, Yang YY. PH-triggered thermally responsive polymer core–shell nanoparticles for drug delivery. Adv Mater 2005;17:318–23.

[39] Wei H, Zhang X-Z, Cheng H, Chen W-Q, Cheng S-X, Zhuo R-X. Self-assembled thermo- and pH-responsive micelles of poly(10-undecenoic acid-b-*N*-isopropylacrylamide) for drug delivery. J Control Release 2006;116:266–74.

[40] Allen C, Maysinger D, Eisenberg A. Nano-engineering block copolymer aggregates for drug delivery. Colloid Surf B Biointerfaces 1999;16:3–27.

[41] Alexandridis P, Holzwarth JF, Hatton TA. Micellization of poly(ethylene oxide)-poly(propylene oxide)-poly(ethylene oxide) triblock copolymers in aqueous solutions: thermodynamics of copolymer association. Macromolecules 1994;27:2414–25.

[42] Astafieva I, Zhong XF, Eisenberg A. Critical micellization phenomena in block polyelectrolyte solutions. Macromolecules 1993;26:7339–52.

[43] Sethuraman A, Han M, Kane RS, Belfort G. Effect of surface wettability on the adhesion of proteins. Langmuir 2004;20:7779–88.

[44] Miller-Chou BA, Koenig JL. A review of polymer dissolution. Prog Polym Sci 2003;28:1223–70.

[45] Huang F, Gibson HW. Polypseudorotaxanes and polyrotaxanes. Prog Polym Sci 2005;30:982–1018.

[46] Han J, Silcock P, McQuillan AJ, Bremera P. Bovine serum albumin adsorption on *N*-methyl-D-glucamine modified colloidal silica. Colloids Surf A Physicochem Eng Aspects 2009;349:207–13.
[47] Bozukova D, Pagnoulle C, De Pauw-Gillet M-C, Ruth N, Robert Jérôme R, Jérôme C. Imparting antifouling properties of poly(2-hydroxyethyl methacrylate) hydrogels by grafting poly(oligoethylene glycol methyl ether acrylate). Langmuir 2008;24:6649–58.